BBA - General Subjects 1866 (2022) 130234

Contents lists available at ScienceDirect

BBA - General Subjects

journal homepage: www.elsevier.com/locate/bbagen

AFM imaging of the transcriptionally active chromatin in mammalian cells' nuclei

V.Yu. Bairamukov [a,*], M.V. Filatov [a], R.A. Kovalev [a], N.D. Fedorova [a], R.A. Pantina [a], A.V. Ankudinov [b], E.G. Iashina [a], S.V. Grigoriev [a], E.Yu. Varfolomeeva [a]

[a] Petersburg Nuclear Physics Institute Named by B.P. Konstantinov of NRC "Kurchatov Institute", 1, Orlova Roshcha, 188300 Gatchina, Russia
[b] The Ioffe Physical-Technical Institute of the Russian Academy of Sciences, 26, Politekhnicheskaya, 194021 Saint Petersburg, Russia

ARTICLE INFO

Keywords:
AFM
Cell nucleus
Chromatin
Mechanical deformation
Transcription
Actinomycin D

ABSTRACT

Background: Nuclear rigidity is traditionally associated with lamina and densely packed heterochromatin. Actively transcribed DNA is thought to be less densely packed. Currently, approaches for direct measurements of the transcriptionally active chromatin rigidity are quite limited.
Methods: Isolated nuclei were subjected to mechanical stress at 60 *g* and analyzed by Atomic Force Microscopy (AFM).
Results: Nuclei of the normal fibroblast cells were completely flattened under mechanical stress, whereas nuclei of the cancerous HeLa were extremely resistant. In the deformed HeLa nuclei, AFM revealed a highly-branched landscape assembled of ~400 nm closed-packed globules and their structure was changing in response to external influence. Normal and cancerous cells' isolated nuclei were strikingly different by DNA resistance to applied mechanical stress. Paradoxically, more transcriptionally active and less optically dense chromatin of the nuclei of the cancerous cells demonstrated higher physical rigidity. A high concentration of the transcription inhibitor actinomycin D led to complete flattening of HeLa nuclei, that might be related to the relaxation of supercoiled DNA tending to deformation. At a low concentration of actinomycin D, we observed the intermediary formation of stochastically distributed nanoloops and nanofilaments with different shapes but constant width ~ 180 nm. We related this phenomenon with partial DNA relaxation, while non-relaxed DNA still remained rigid.
Conclusions: The resistance to deformation of nuclear chromatin correlates with fundamental biological processes in the cell nucleus, such as transcription, as assessed by AFM.
General significance: A new outlook to studying internal nuclei structure is proposed.

1. Introduction

In mammalian cell nuclei, DNA is highly packed and stored, being involved in the central biological processes, in particular, transcription. The transcriptional profile at tumorigenesis is significantly changed compared to normal tissues [1]. As a result, nuclei of cancerous cells are very heterogeneous by size and shape. While pathognomonic changes in morphology in the cancer nucleus were evaluated in the early 19th century by Follin [2], in the last decade a variety of diseases are associated with aberrant cell nuclear mechanics [3,4].

Nuclear mechanics is traditionally related to the exterior lamina and interior chromatin. The lamina surface stiffness is measured by AFM as a local stiffness of the nuclear region of an intact cell [5,6], by chemical removal of extranuclear component [7], or in situ in an isolated nucleus [8,9]. The nucleus filled in with chromatin is inaccessible for direct measurements. Historically, chromatin is divided into compactly organized heterochromatin and euchromatin, deployed during transcription. Heterochromatin is most abundant at the nuclear periphery [10], closely associated with the nuclear lamina through association with integral nuclear membrane (INM) [11]. Most of the studies stated a primary role of heterochromatin in nuclear mechanics. By using optical tweezers, it has been shown that chromatin in nuclei, lacking INM tethers, is less stiff, than in wild-type nuclei and exhibits increased chromatin flow [12]. In another study with optical tweezers micromanipulation, the authors observed, that the small-strain nuclear elasticity of chromatin could be affected by the modification of histones [13]. It was shown that hyperacetylation led to a softer mechanical response, whereas increased heterochromatin ratio led to stiffer ones. In the review [14], the authors

* Corresponding author.
E-mail address: bayramukov_vy@pnpi.nrcki.ru (V.Yu. Bairamukov).

https://doi.org/10.1016/j.bbagen.2022.130234
Received 16 May 2022; Received in revised form 21 July 2022; Accepted 18 August 2022
Available online 22 August 2022

suggested that condensed chromatin possesses a significant elastic rigidity and could act not only as storage of genetic information, but be involved in the mechanical response. Later, it has been reported that an increase in heterochromatin ratio led to an increase in chromatin-based nuclear rigidity and suppresses nuclear blebbing through activation of mechanosensitive ion channels at different Mg^{2+} concentrations [15].

However, gene expression in the mammalian cells' nuclei is excluded from the periphery, hence transcription is implicated in euchromatin organization [16]. As suggested by recent theoretical work, gene expression is highly correlated and tightly regulated by supercoiling, which depends on DNA unwinding by polymerases [17]. Later on, the basic physical elements of transcription were proposed, where RNA elongation, polymerase rotation and DNA supercoiling are coupled [18]. The question about the contribution of those transcription factories to nuclear rigidity is still obscured. Recent work sheds light on the relationships between nuclear mechanics and transcription [19]. Nuclei isolated from cancerous cells were studied by AFM micro-rheology and showed similar qualitative behavior consisting of their softer and more viscous response towards the nuclear periphery. The authors suggested a reduced degree of crosslinking of the chromatin, which is achieved through condensation by condensin protein complexes. These results indicated, that various levels of DNA condensation may exist.

Here we showed that normal and cancerous cells' nuclei were drastically distinguished by resistance to applied mechanical stress. Though nuclei isolated from normal cells were basically flattened, while the cancerous ones demonstrated a highly-branched landscape that rose up a hundred nanometers above the substrate, and was assembled in globules. We proposed that the difference might be attributed to some of the fundamental biological processes in the cell nucleus, such as transcription. In order to test this, we analyzed the effects of different concentrations of the primary transcription inhibitor actinomycin D. HeLa cells incubation with transcription inhibitor prior to the mechanical stress application resulting in transformation of closed-packed globules into multiple-shaped nanoloops and nanofilaments. These results indicated that closed-packed globules might be associated with transcriptionally active chromatin domains and be in the supercoiled state. The tension of the supercoiled DNA could be gradually relaxed as transcription was inhibited, eventually leading to the complete flattening of HeLa nuclei. The results suggest that the concept of the contribution of transcription active chromatin to nuclear rigidity could be reconsidered.

2. Methods

2.1. Nuclei isolation

In our study, a normal cell line of human embryo lung diploid fibroblasts and cancerous HeLa cell lines were used. The cell lines were obtained from the Cell Culture Collection of the Institute of Cytology of the Russian Academy of Sciences, St. Petersburg, Russia. Cells were cultured at 37C with 5% CO_2 in DMEM/F12 medium supplemented with 10% fetal bovine serum.

HeLa cells were incubated with transcription inhibitor actinomycin D at the stage of cells growth at different concentration ranges: 0.03 and 0.12 μg/ml for a day; 0.12 μg/ml for two days.

The samples of chicken erythrocytes nuclei were obtained by isolation of the nuclei from the chicken red blood cells as we described previously [20]. Briefly, the whole blood was centrifuged at the spin centrifuge for 10 min at 170 rcf. The supernatant, containing plasma proteins, was removed and the resulting precipitate was resuspended in a standard PBS buffer with 6 mM EDTA. The washing procedure was repeated three times. The resulting red blood cells were lysed as described below for human fibroblasts nuclei and HeLa nuclei.

Human fibroblasts nuclei and HeLa nuclei were isolated from cells according to the reproducible protocol described previously [21]. Briefly, cells were washed with 10 ml of Versene Solution and centrifuged at the spin centrifuge for 10 min at 170 rcf. to remove supernatant. Nuclei were lysed within 5 min with 0.15% Triton-X100 in culture medium DMEM/F12 with 15 mM HEPES Buffer. Triton-X100 concentration and the time exposure we used, let us to dissolve the cell membrane and preserve the nucleus membrane.

2.2. Nuclei immobilization onto the substrate

As a substrate for nuclei immobilization microscope slide (26 × 76 mm / ca. 1 mm) covered with poly-L-lysine was used. The microscope slide was intensively washed in ethanol and rinsed with Milli-Q. After drying on air microscope slide was covered by 0.001 wt% of poly-L-lysine solution, stored for 5 min, rinsed with Milli-Q and dried at room temperature. The roughness of the substrate according to AFM was 14 ± 6 nm.

The first part of the freshly lysed nuclei was fixed in solution with 0.5 wt% of glutaraldehyde for 10 min via intensive pipetting and 1 μl of the suspension was dispensed onto a substrate. After 10 min of incubation, the substrate was extensively washed with Milli-Q and left drying overnight.

2.3. Mechanical deformation

The second part of the freshly lysed nuclei was not fixed in suspension, and 1 μl of it was dispersed onto the substrate, which was immediately placed in a Petri dish and it carefully placed in S750—6B bucket rotor (Hanil Scientific Inc.) of UNION 5 K centrifuge and centrifuged at its minima of 500 rpm (60 *g*) for 5 min at room temperature. After the procedure, deformed nuclei were immediately fixed with 0.5 wt% glutaraldehyde for 10 min and then extensively rinsed with Milli-Q. The samples were left drying overnight.

2.4. AFM measurements

AFM measurements were carried out at NTEGRA Spectra II atomic force microscope (NT-MDT, Russia) equipped with an optic microscope. NSG03 tips (NT-MDT, Russia) with tip radius 10 nm and spring constant 2 N/m were used in tapping mode. The scan rate was 0.6 Hz and the resonance frequency was 79 kHz with a tapping amplitude of 30 nm. Images processed in Gwyddion 2.55 software. Nuclear volume and fractal dimension (Cube counting) were calculated in Gwyddion 2.55 software using embedded program algorithms.

3. Results

Mammalian cell nuclei can be isolated from cells, fixed in suspension and, when placed onto a substrate, becomes near-spherical shape. Obviously, in this way, AFM cannot be applicable to investigate nuclear internal structure. However, if the isolated nuclei were not fixed, but placed onto a substrate and underwent mechanical deformation, the peculiarities of the internal structure organization are transformed into a landscape, resistant to deformation. Fixation with glutaraldehyde makes the deformed nuclei accessible for subsequent study by AFM.

We first compared alteration in morphology of normal cell nuclei (human fibroblasts), and rudimentary chicken erythrocytes in response to mechanical deformation. It is well established that in chicken erythrocytes the bulk of the genome is highly compacted and silent [22]. Nuclei fixed in suspension and placed onto a substrate were characterized only by varying their near-spherical shape. Here we could estimate the size of nuclei for each AFM image below (Fig. 1a, 1c). Applied mechanical stress led to the deformation of the nuclear interior, forming flattened objects, enlarged in lateral sizes at several micrometers (Fig. 1b, d). Please note that it is a top view, and the height is given in nanometers. In deformed fibroblasts, appeared nuclear interior components became resistant to deformation, varying by quantity and size distribution. The most prominent features were up to ~300 nm in height and 1–1.5 μm in diameter. We associated them with nucleoli (enlarged

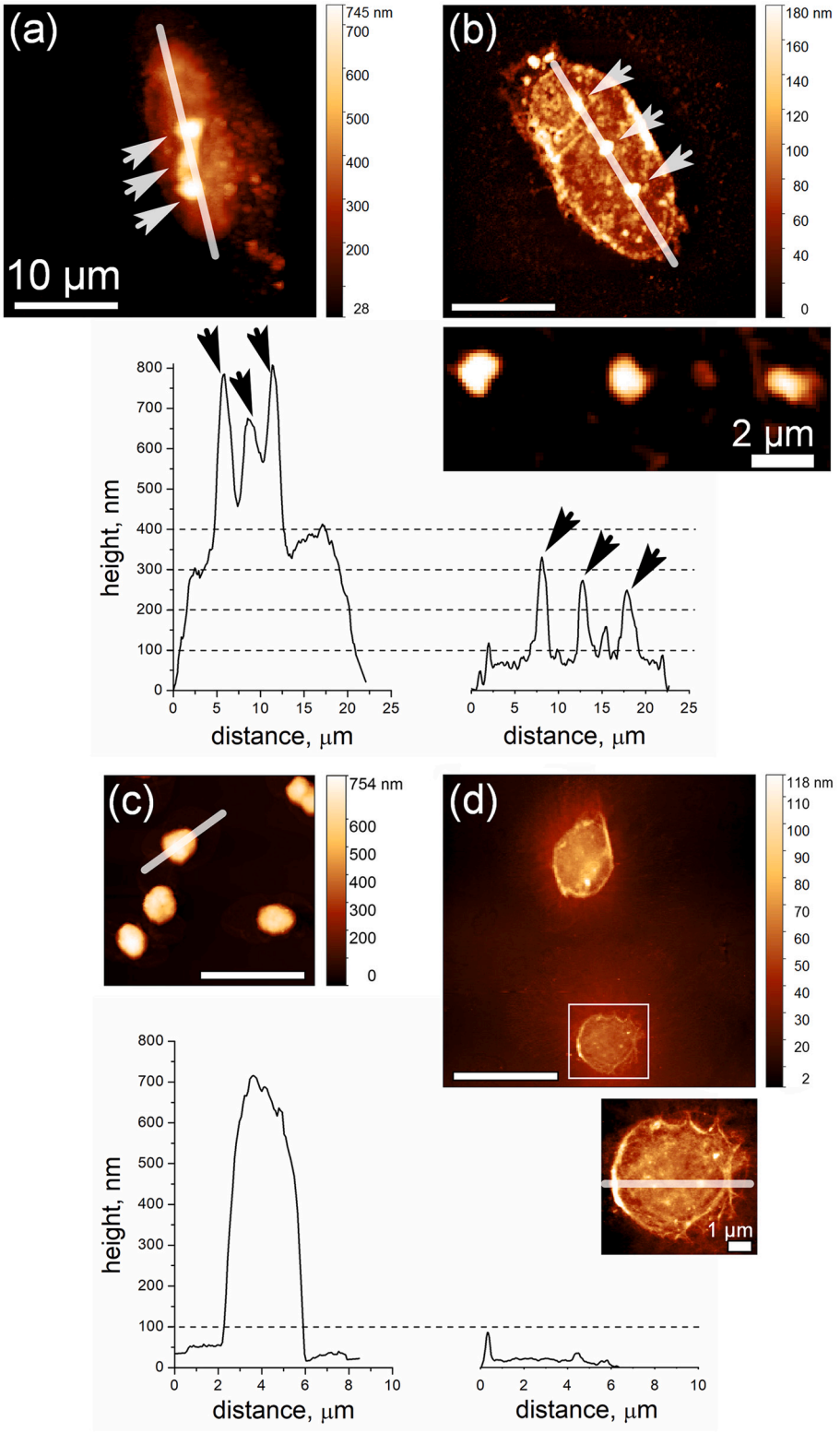

Fig. 1. AFM images of human fibroblasts nucleus and chicken erythrocytes nuclei fixed in suspension (a, c) and undergone mechanical deformation (b, d). The scale bar is 10 μm. The profile of the nucleus is given below the corresponding image.

area below Fig. 1b). Typically, normal nuclei contain 1–3 nucleoli. In the completely flattened chicken erythrocytes nuclei, nucleoli did not appear (Fig. 1d).

More examples of discussed flattened nuclei with the top view and 3D view are given in Supplementary Figs. 1 and 2. Please note, that our previously studied rat lymphocytes nuclei demonstrated similarities with fibroblasts under mechanical deformation varying by the number of nucleoli and shape [23].

A completely different distribution of nuclear chromatin after mechanical deformation was observed at cancerous HeLa cells' nuclei, characterized by aberrant gene expression. AFM image of the isolated nucleus, fixed in suspension and placed onto the substrate, is presented

in Fig. 2a. Typically, HeLa nuclei, fixed in suspension, rose up above substrate at 800–1000 nm with prominent features up to 1200–1600 nm. Surprisingly, after applied mechanical stress, nuclear chromatin stayed resistant to deformation (Fig. 2b). A highly-branched landscape, rising up above the substrate at 150–250 nm and prominent nucleoli up to 400–500 nm were revealed. In the nuclei of cancer cells, the nucleoli' size and their number are typically increased [24]. The size, quantity, and distribution of the nucleoli may vary in nuclei, although chromatin remains resistant to deformation as also shown in Supplement Fig. 3. A comparison of the morphology of nucleoli and resistant nuclear chromatin revealed structural differences. The morphology of ribonucleoprotein (RNP) nucleolus was amorphous, consisting of randomly block-chained domains, whereas resistant nuclear chromatin consisted of ~400 nm granular units. In our observation, lateral broadening due to the co-sedimented component of the nuclear membrane should be considered. Taking this into account, the data are correlated with AFM study of on-substrate lysis of HeLa nuclei [25]. In that work, after the extraction of the nuclear membrane of isolated nuclei the authors observed 80–100 nm bead structures that were associated with a one-step higher architecture of chromatin. Nevertheless, our results suggest that larger beads-like units could be associated with DNA supercoiled state involved in transcription. In support of this interpretation, incubation of the HeLa cells with a transcription inhibitor that reduces DNA supercoiling and relaxes tensions results in nuclei chromatin tendency to deformation. We applied actinomycin D at a concentration of 0.12 μg/ml for 2 days. Actinomycin is considered a compound that behaves both as a DNA intercalator and a minor groove binding agent [26]. It intercalates between the G-C step forming a very stable

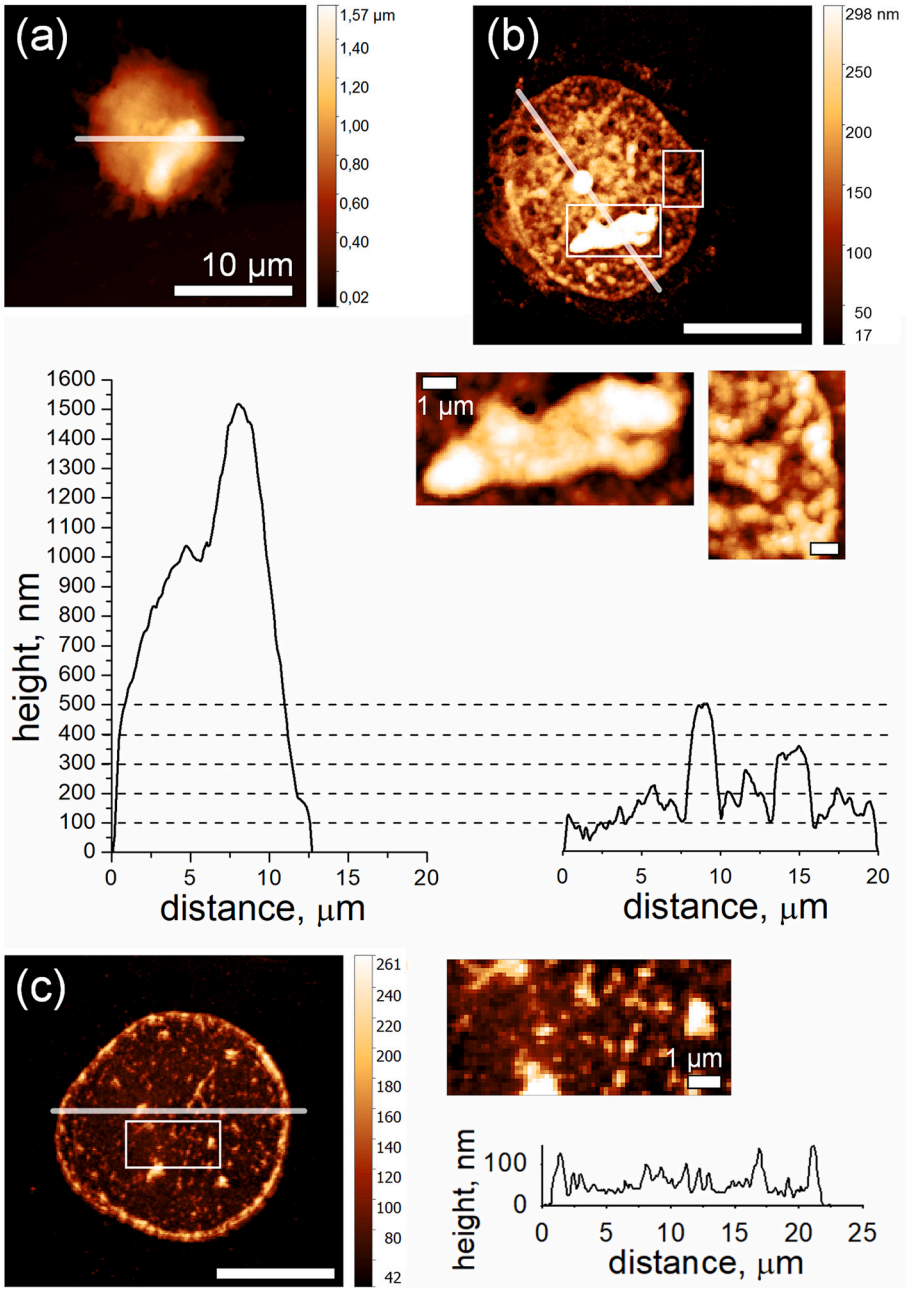

Fig. 2. AFM images of HeLa nuclei: (a) – fixed in suspension, (b) – mechanically deformed, and (c) – cells were treated with 0.12 μg/ml of actinomycin D for 2 days followed by nuclei isolation and mechanical deformation. The scale bar is 10 μm. The profile of the nucleus is below the corresponding image. In the enlarged areas, the scale bar is 1 μm.

actinomycin–DNA complex and inhibits the DNA-dependent RNA polymerase activity, thus preventing transcription and reducing the DNA supercoiling. [27,28]. It also generates double-strand breaks in DNA, similar to double-strand breaks induced by topoisomerase II inhibitors [29]. Our results to this point are presented in Fig. 2c. As was expected, actinomycin D treatment led to a relaxation of DNA tensions, and nuclear chromatin generally deformed in response to the mechanical stress. It is also known that under actinomycin D treatment nucleoli even disappeared or drastically decreased in size [30] (Supplement Fig. 4).

Next, if treatment time and concentration of actinomycin D are reduced, remarkable structural features in deformed nuclei appear. Their sizes lie beyond the resolution of optic microscopy. Qualitatively, we tried to evaluate changes in morphology using the fractal analysis of AFM images [31].

In Fig. 3a, for isolated and mechanically deformed HeLa nucleus, the fractal dimension of the globular-consisted area was calculated as being 2.304. After treatment of cells with actinomycin D with a concentration of 0.03 μg/ml for 1 day overlapped multiple loops predominantly 1 μm in diameter span the whole nucleus appeared (Fig. 3b). The increase of the branching of the surface from closed-packed globules to branched loops is reflected by the increase of fractal dimension at 2.383. Finally, after treatment of cells with actinomycin D with a concentration of 0.12 μg/ml for 1 day, stochastically distribution of single nanoloops and nanofilaments with terminal width of ~160–180 nm was observed (Fig. 3c). Correspondingly, the fractal dimension decreased at 2.299 which indicated a decrease in the amount of resistant nuclear chromatin. Notably, the distribution of those structures in nuclei was always diverse (Supplement Fig. 5).

The observed differences in actinomycin D time exposure (Figs. 2c and 3c) could be associated with different actions of transcription

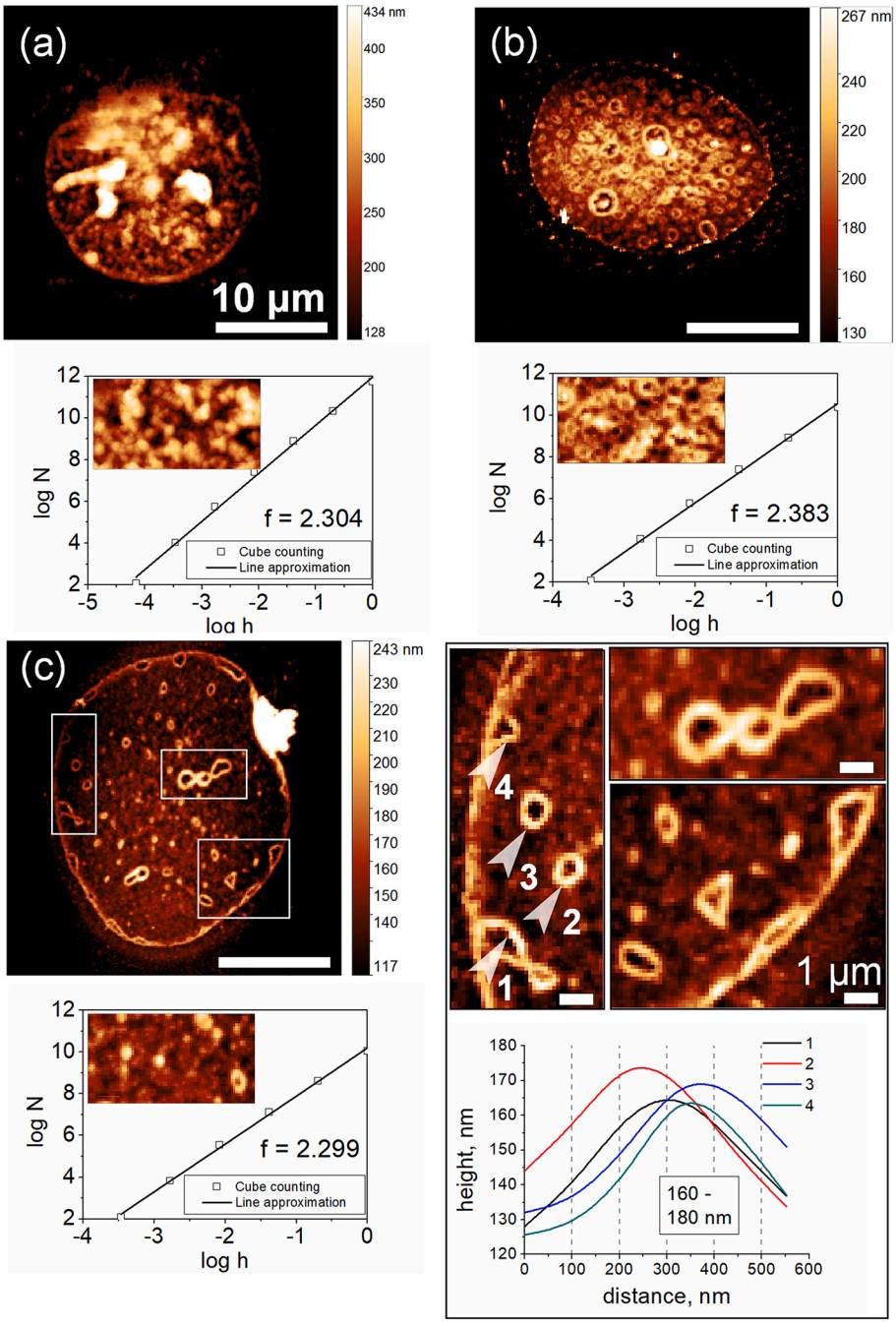

Fig. 3. AFM images of deformed HeLa nucleus: (a) – no actinomycin D treatment, (b) – treatment with 0.03 μg/ml, and (c) – 0.12 μg/ml of actinomycin D. Exposure time for (b) and (c) was 1 day. The scale bar is 10 μm. The calculated fractal dimension of area 4.5 × 8.5 μm is below the corresponding image. An increase in fractal dimension reflects an increase in the branching of the morphology. On the right of Fig. 3c, enlarged areas with nanoloops and nanofilaments with calculated diameters were given.

inhibitor. In Fig. 2c, an excess of the compound generated DNA double-strand breaks. By comparison, in our previous experiments, HeLa cells were incubated with topoisomerases inhibitors I and II (camptothecin and etoposide, respectively). After nuclei deformation, their complete flattening was demonstrated, while the RNP nucleoli were preserved [32]. Also, in numerous experiments, we did not observe nanoloops and nanofilaments.

On the contrary, actinomycin D acts as an intercalator (Fig. 3c) and down-regulates transcription by arresting RNA polymerases, inducing partial DNA relaxation. If actinomycin D was removed from the cells' environment, transcription activity recovered within about 16 h (Supplement Fig. 6). Notably, Ethidium Bromide (EtBr) is another DNA intercalator, which inserts between the stacked bases in DNA increasing the persistent length of the double helix [33]. DNA begins to wrap again but in the opposite direction. Treatment of HeLa nuclei with EtBr followed by mechanical deformation revealed increasing in DNA rigidity [32].

Consequently, all these manipulations demonstrate a relationship between DNA state and nuclear mechanics, that can be revealed by applied mechanical stress.

4. Discussion

The cell nucleus contains an extremely large amount of macromolecule compounds i.e., DNA, RNA, and proteins. The concentration of these compounds is so high that it is difficult, if not impossible, to artificially generate such a concentrated solution. According to the estimates, the total concentration of macromolecules in the nucleus could exceed 100 mg/ml [34,35]. Any non-biological formations containing such high concentrations of macromolecules would be extremely viscous and be an elastic gel, resistant to deformation. It should be assumed, that the organization of the material of the nucleus is largely unique, which may be associated with a significant decrease in viscosity. Instead it has been established, that nucleus, even if put onto the substrate or held without fixation for a short time, revealed its internal morphological peculiarities [36,37].

Recently we have described for the first time an alteration in morphology in response to mechanical stress for chicken erythrocyte [20], HeLa [21], and rat lymphocyte nuclei [23], and confirmed the integrity of the nuclei by flow cytometry. Previously, we focused on the analysis of microstructure by small-angle neutron scattering (SANS). SANS demonstrated the bi-fractal nature of the chromatin structural organization in all the above-mentioned nuclei. The scattering intensity is described by power law Q^{-D} with exponent 2.4 on smaller scales and with exponent 3 on larger scales. The exponent D = 2.4 corresponded to the mass fractal on the scale from ten to sometimes hundreds nanometers, while exponent D = 3 is attributed to the logarithmic fractal on the scale from hundred nanometers to ten micrometers. Thus, the hypothesis of the bi-fractal structure of chromatin in the interphase nucleus was proposed. In an attempt to identify the two fractal levels of the chromatin differentiated in the SANS experiment, the combined analysis of the SANS and AFM was performed. The analysis provided evidence for the two types of chromatin with different physical (dense or loose; soft or rigid) and fractal (power function or logarithmic function) properties. It was shown for all the cell lines under study, that their nuclei were quizzed till the height was practically equal to the crossover value between two fractal levels. The height of these flattened nuclei assessed by AFM coincided closely with the fractal borderline, thus characterizing a type of chromatin at a smaller scale as being rigid and ones, at a larger scale, as being soft. We correlated the mechanical properties (rigid or soft) obtained from AFM and the fractal properties (loose or dense) obtained from SANS. Combining the results of SANS and AFM measurements, one concluded that the chromatin in nuclei is characterized as a rigid, loosely packed, mass fractal at a smaller scale, and as a soft, densely packed logarithmic fractal at a larger scale. We, therefore, could further conclude that AFM study of the surface of the nuclei deformed by centrifugation is relevant for the identification of the fractal properties of nuclei that is, in the range of the mass (volume) fractal, clearly determined by SANS.

Here, in view of AFM, we attempted to classify nuclei according to their resistance to deformation in response to external influence, describe structural features that were observed, and generally speculate about the origin of that phenomenon.

In numerous experiments, we observed that the nuclei of normal cells, such as human fibroblasts or rat lymphocytes [23], are more prone to deformation compared to HeLa cells nuclei. This may imply that active transcription may provide a basis for a correlation between the nuclear rigidity and the amount of supercoiled DNA. To estimate the contribution of soft and rigid DNA to the nuclei filled interior we compared the volumes of nuclei fixed in suspension and ones that underwent mechanical deformation (Fig. 4).

The average value of the calculated volume of HeLa nuclei fixed in suspension state was 80.39 ± 20.08 μm^3 and differed by 1.4 times compared to ones that underwent mechanical deformation (53.64 ± 15.71 μm^3). Notably, in the experiments carried out at HeLa nuclei, chromatin stayed resistant even under 2000 rpm. On the contrary, from fibroblasts fixed in suspension, the calculated volume was 53.75 ± 10.37 μm^3 and differed by 2.8 times compared to ones underwent mechanical deformation (18.91 ± 5.38 μm^3). It indicated that HeLa nuclei might contain a lot more supercoiled DNA which does not allow changing of nuclear volume. Consequently, nuclear rigidity could be determined not only by a stiff lamina and optically dense heterochromatin, but also transcriptionally active chromatin. In our experiments, the results demonstrated that more transcriptionally active and less optically dense chromatin of the cancerous nuclei possessed higher physical rigidity. Following this logic, the results correlate with ones of quantitative estimation of rigidity based on the Young's modulus calculation [19] and strictly point out the relationships between nuclear mechanics and transcription.

It is tempting to speculate that the observed nanoloops and nanofilaments are associated with transcription factories. It was suggested that transcription occurs at discrete sites in the nucleus being 100 nm or less [38,39]. In those sites, multiple active RNA polymerases are concentrated and anchored to a nuclear sub-structure [40] and stochastically appear in nuclei [17]. It was recently shown that physical contact between DNA and RNA that is established by RNA polymerase is required to maintain the interspersed pattern of DNA and RNA domains. The dissociation of DNA-RNA contacts results in DNA coarsening. In the recently published [41] it was shown no detectable coarsening of the DNA domains occurred upon actinomycin D treatment. According to the estimates, transcription could be characterized by its own mechanical

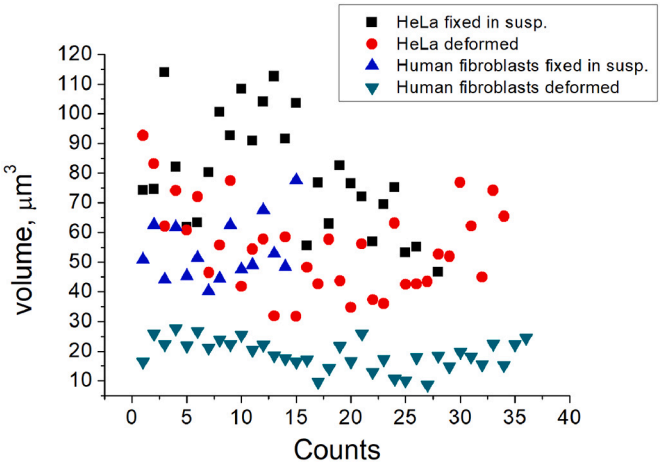

Fig. 4. Volume distribution of human fibroblasts (n = 51) and HeLa nuclei (n = 63) fixed in suspension and underwent mechanical deformation.

parameters [18]. Quantitative mechanical characterization of the observed nuclear features is obscured by the strong surface fixation with glutaraldehyde. Nevertheless, we can qualitatively estimate, that the nanoloops and nanofilaments that we observe, are stochastically distributed and characterized by a constant width. It should be taken into account, that the size of the peculiarities might be increased due to co-sedimentation of the nuclear membrane component under mechanical deformation.

5. Conclusion

Here we describe the method to transform the inhomogeneities of the nuclear interior organization into the surface landscape via mechanical stress, thus, making the nuclear landscape accessible for AFM. Employing this approach, we were able to capture the changes in morphology that correlate with functional processes in the cell nucleus.

Supplementary data to this article can be found online at https://doi.org/10.1016/j.bbagen.2022.130234.

Author contributions

The manuscript was written with the contributions of all authors. All authors have given approval to the final version of the manuscript and have no conflict of interests.

Funding

The reported study was funded by the Russian Science Foundation under Grant 20–12-00188.

Declaration of Competing Interest

The authors declare that they have no known competing financial interests or personal relationships that could have appeared to influence the work reported in this paper.

Data availability

Data will be made available on request.

Acknowledgement

The authors are grateful to Dr. Vladimir V. Isaev-Ivanov for providing the experimental time for the initial experiments and to Dr. Evgeny M. Makarov for criticism, that improved the manuscript. We also grateful to Dr. Olga G. Shcherbakova for carefully reading the manuscript.

References

[1] D.K. Slonim, Transcriptional profiling in cancer: the path to clinical pharmacogenomics, Pharm. J. 2 (2001) 123–136, https://doi.org/10.1517/14622416.2.2.123.
[2] V.A. Triolo, Nineteenth century foundations of cancer research advances in tumor pathology, nomenclature, and theories of oncogenesis, Cancer Res. 25 (1965) 75–106 (PMID: 14264062).
[3] C. Denais, J. Lammerding, Nuclear mechanics in cancer, Adv. Exp. Med. Biol. 773 (2014) 435–470, https://doi.org/10.1007/978-1-4899-8032-8_20.
[4] A.D. Stephens, Nucleus|Chromatin and Nuclear Biophysics, in: J. Jez (Ed.), Encyclopedia of Biological Chemistry III, Third edition, Elsevier, 2021, pp. 372–378, https://doi.org/10.1016/B978-0-12-819460-7.00272-3.
[5] M. Krause, J. te Riet, K. Wolf, Probing the compressibility of tumor cell nuclei by combined atomic force-confocal microscopy, Phys. Biol. 10 (2013), 065002, https://doi.org/10.1088/1478-3975/10/6/065002.
[6] J. Schäpe, S. Prauße, M. Radmacher, R. Stick, Influence of Lamin a on the mechanical properties of amphibian oocyte nuclei measured by atomic force microscopy, Biophys. J. 96 (2009) 4319–4325, https://doi.org/10.1016/j.bpj.2009.02.048.
[7] K. Wang, Y. Qin, Y. Chen, In situ AFM detection of the stiffness of the in situ exposed cell nucleus, Biochim. Biophys. Acta, Mol. Cell Res. 1868 (2021), 118985, https://doi.org/10.1016/j.bbamcr.2021.118985.
[8] H.J. Liu, J. Wen, Y. Xiao, J. Liu, S. Hopyan, M. Radisic, C.A. Simmons, Y. Sun, In situ mechanical characterization of the cell nucleus by atomic force microscopy, ACS Nano 8 (2014) 3821–3828, https://doi.org/10.1021/nn500553z.
[9] T. Sugitate, T. Kihara, X.-Y. Liu, J. Miyake, Mechanical role of the nucleus in a cell in terms of elastic modulus, Curr. Appl. Phys. 9 (2009) e291–e293, https://doi.org/10.1016/j.cap.2009.06.020.
[10] E. Deniaud, W.A. Bickmore, Transcription and the nuclear periphery: edge of darkness? Curr. Opin. Genet. Dev. 19 (2009) 187–191, https://doi.org/10.1016/j.gde.2009.01.005.
[11] Y. Gruenbaum, A. Margalit, R.D. Goldman, D.K. Shumaker, K.L. Wilson, The nuclear lamina comes of age, Nat. Rev. Mol. Cell Biol. 1 (2005) 21–31, https://doi.org/10.1038/nrm1550.
[12] S. Schreiner, P. Koo, Y. Zhao, S.G.J. Mochrie, M.C. King, The tethering of chromatin to the nuclear envelope supports nuclear mechanics, Nat. Commun. 6 (2015) 7159, https://doi.org/10.1038/ncomms8159.
[13] A.D. Stephens, E.J. Banigan, S.A. Adam, R.D. Goldman, J.F. Marko, Chromatin and Lamin a determine two different mechanical response regimes of the cell nucleus, Mol. Biol. Cell 28 (2017) 1984–1996, https://doi.org/10.1091/mbc.E16-09-0653.
[14] K. Maeshima, S. Tamura, Y. Shimamoto, Chromatin as a nuclear spring 15, BPPB, 2018, pp. 189–195, https://doi.org/10.2142/biophysico.15.0_189.
[15] A.D. Stephens, P.Z. Liu, V. Kandula, H. Chen, L.M. Almassalha, C. Herman, V. Backman, T. O'Halloran, S.A. Adam, R.D. Goldman, E.J. Banigan, J.F. Marko, Physicochemical mechanotransduction alters nuclear shape and mechanics via heterochromatin formation, Mol. Biol. Cell 30 (2019) 2320–2330, https://doi.org/10.1091/mbc.E19-05-0286.
[16] J.M. Levsky, S.M. Shenoy, J.R. Chubb, C.B. Hall, P. Capodieci, R.H. Singer, The spatial order of transcription in mammalian cells, J. Cell. Biochem. 102 (2007) 609–617, https://doi.org/10.1002/jcb.21495.
[17] C.A. Brackley, J. Johnson, A. Bentivoglio, S. Corless, N. Gilbert, G. Gonnella, D. Marenduzzo, Stochastic model of supercoiling-dependent transcription, Phys. Rev. Lett. 117 (2016), 018101, https://doi.org/10.1103/PhysRevLett.117.018101.
[18] S.A. Sevier, H. Levine, Mechanical properties of transcription, Phys. Rev. Lett. 118 (2017), 268101, https://doi.org/10.1103/PhysRevLett.118.268101.
[19] M. Lherbette, Á. Dos Santos, Y. Hari-Gupta, N. Fili, C.P. Toseland, I.A.T. Schaap, Atomic force microscopy micro-rheology reveals large structural inhomogeneities in single cell-nuclei, Sci. Rep. 7 (2017) 8116, https://doi.org/10.1038/s41598-017-08517-6.
[20] S.V. Grigoriev, E.G. Iashina, V.Y. Bairamukov, V. Pipich, A. Radulescu, M. V. Filatov, R.A. Pantina, E.Y. Varfolomeeva, Switch of fractal properties of DNA in chicken erythrocytes nuclei by mechanical stress, Phys. Rev. E 102 (2020), 032415, https://doi.org/10.1103/PhysRevE.102.032415.
[21] S.V. Grigoriev, E.G. Iashina, B. Wu, V. Pipich, Ch. Lang, A. Radulescu, V. Yu. Bairamukov, M.V. Filatov, R.A. Pantina, E.Yu. Varfolomeeva, Observation of nucleic acid and protein correlation in chromatin of HeLa nuclei using small-angle neutron scattering with D 2 O − H 2 O contrast variation, Phys. Rev. E 104 (2021), 044404, https://doi.org/10.1103/PhysRevE.104.044404.
[22] S. Jahan, W. Xu, S. He, C. Gonzalez, G.P. Delcuve, J.R. Davie, The chicken erythrocyte epigenome, Epigenetics Chromatin 9 (2016) 19, https://doi.org/10.1186/s13072-016-0068-2.
[23] E.G. Iashina, E.Y. Varfolomeeva, R.A. Pantina, V.Y. Bairamukov, R.A. Kovalev, N. D. Fedorova, V. Pipich, A. Radulescu, S.V. Grigoriev, Bifractal structure of chromatin in rat lymphocyte nuclei, Phys. Rev. E 104 (2021), 064409, https://doi.org/10.1103/PhysRevE.104.064409.
[24] D. Zink, A.H. Fischer, J.A. Nickerson, Nuclear structure in cancer cells, Nat. Rev. Cancer 9 (2004) 677–687, https://doi.org/10.1038/nrc1430.
[25] T. Kobori, M. Kodama, K. Hizume, S.H. Yoshimura, T. Ohtani, K. Takeyasu, Comparative structural biology of the genome: nano-scale imaging of single nucleus from different kingdoms reveals the common physicochemical property of chromatin with a 40 nm structural unit, J. Electron Microsc. 55 (2006) 31–40, https://doi.org/10.1093/jmicro/dfi076.
[26] C. Avendaño, J.C. Menéndez, DNA Intercalators and topoisomerase inhibitors, in: C. Avendano, J.C. Menendez (Eds.), Medicinal Chemistry of Anticancer Drugs, Elesevier BV, Oxford, 2008, pp. 199–228, https://doi.org/10.1016/B978-0-444-52824-7.00007-X.
[27] D.K. Trask, M.T. Muller, Stabilization of type I topoisomerase-DNA covalent complexes by actinomycin D, Proc. Natl. Acad. Sci. U. S. A. 85 (1988) 1417–1421, https://doi.org/10.1073/pnas.85.5.1417.
[28] B. Borsos, I. Huliák, H. Majoros, Z. Ujfaludi, Á. Gyenis, P. Pukler, I.M. Boros, T. Pankotai, Human p53 interacts with the elongating RNAPII complex and is required for the release of actinomycin D induced transcription blockage, Sci. Rep. 7 (2017) 40960, https://doi.org/10.1038/srep40960.
[29] W.E. Ross, M.O. Bradley, DNA double-stranded breaks in mammalian cells after exposure to intercalating agents, Biochim. Biophys. Acta 654 (1981) 129–134, https://doi.org/10.1016/0005-2787(81)90145-3.
[30] B. Kramer, The effect of actinomycin D on the nucleolus and on pigment synthesis in pigment cells of Xenopus laevis: an ultrastructural study, J. Anat. 130 (Pt 4) (1980) 809–820 (PMID: 7429969).
[31] A. Bitler, R.S. Dover, Y. Shai, Fractal properties of cell surface structures: a view from AFM, Semin. Cell Dev. Biol. 73 (2018) 64–70, https://doi.org/10.1016/j.semcdb.2017.07.034.
[32] V.Yu. Bairamukov, M.V. Filatov, R.A. Kovalev, R.A. Pantina, S.V. Grigoriev, E. Yu. Varfolomeeva, Structural peculiarities of mechanically deformed HeLa nuclei revealed by atomic force microscopy, J. Surf. Investig. 16 (2022) 854–859, https://doi.org/10.1134/S1027451022050263.

[33] S. Husale, W. Grange, M. Hegner, DNA mechanics affected by small DNA interacting ligands, Single Mol. 3 (2002) 91–96, https://doi.org/10.1002/1438 5171(200206)3:2/3%3C91::AID-SIMO91%3E3.0.CO;2-R.
[34] R. Hancock, A role for macromolecular crowding effects in the assembly and function of compartments in the nucleus, J. Struct. Biol. 146 (2004) 281–290, https://doi.org/10.1016/j.jsb.2003.12.008.
[35] R. Hancock, Internal organization of the nucleus: assembly of compartments by macromolecular crowding and the nuclear matrix model, Biol. Cell. 96 (2004) 595–601, https://doi.org/10.1016/j.biolcel.2004.05.003.
[36] Y. Hirano, H. Takahashi, M. Kumeta, K. Hizume, Y. Hirai, S. Otsuka, S. H. Yoshimura, K. Takeyasu, Nuclear architecture and chromatin dynamics revealed by atomic force microscopy in combination with biochemistry and cell biology, Pflugers Arch. 456 (2008) 139–153, https://doi.org/10.1007/s00424-007-0431-z.
[37] V.V. Isaev-Ivanov, D.V. Lebedev, H. Lauter, R.A. Pantinaa, A.I. Kuklind, A. Kh. Islamovd, M.V. Filatov, Comparative analysis of the nucleosome structure of cell nuclei by small-angle neutron scattering, Phys. Solid State 52 (2010) 1063–1073, https://doi.org/10.1134/S1063783410050379.
[38] F.J. Iborra, A. Pombo, D.A. Jackson, P.R. Cook, Active RNA polymerases are localized within discrete transcription 'factories' in human nuclei, J. Cell Sci. 109 (1996) 1427–1436, https://doi.org/10.1242/jcs.109.6.1427.
[39] P.R. Cook, The organization of replication and transcription, Science. 284 (1999) 1790–1795, https://doi.org/10.1126/science.284.5421.1790.
[40] H. Sutherland, W.A. Bickmore, Transcription factories: gene expression in unions? Nat. Rev. Genet. 10 (2009) 457–466, https://doi.org/10.1038/nrg2592.
[41] L. Hilbert, Y. Sato, K. Kuznetsova, T. Bianucci, H. Kimura, F. Jülicher, A. Honigmann, V. Zaburdaev, N.L. Vastenhouw, Transcription organizes euchromatin via microphase separation, Nat. Commun. 12 (2021) 1360, https://doi.org/10.1038/s41467-021-24517-7.

Supplementary information

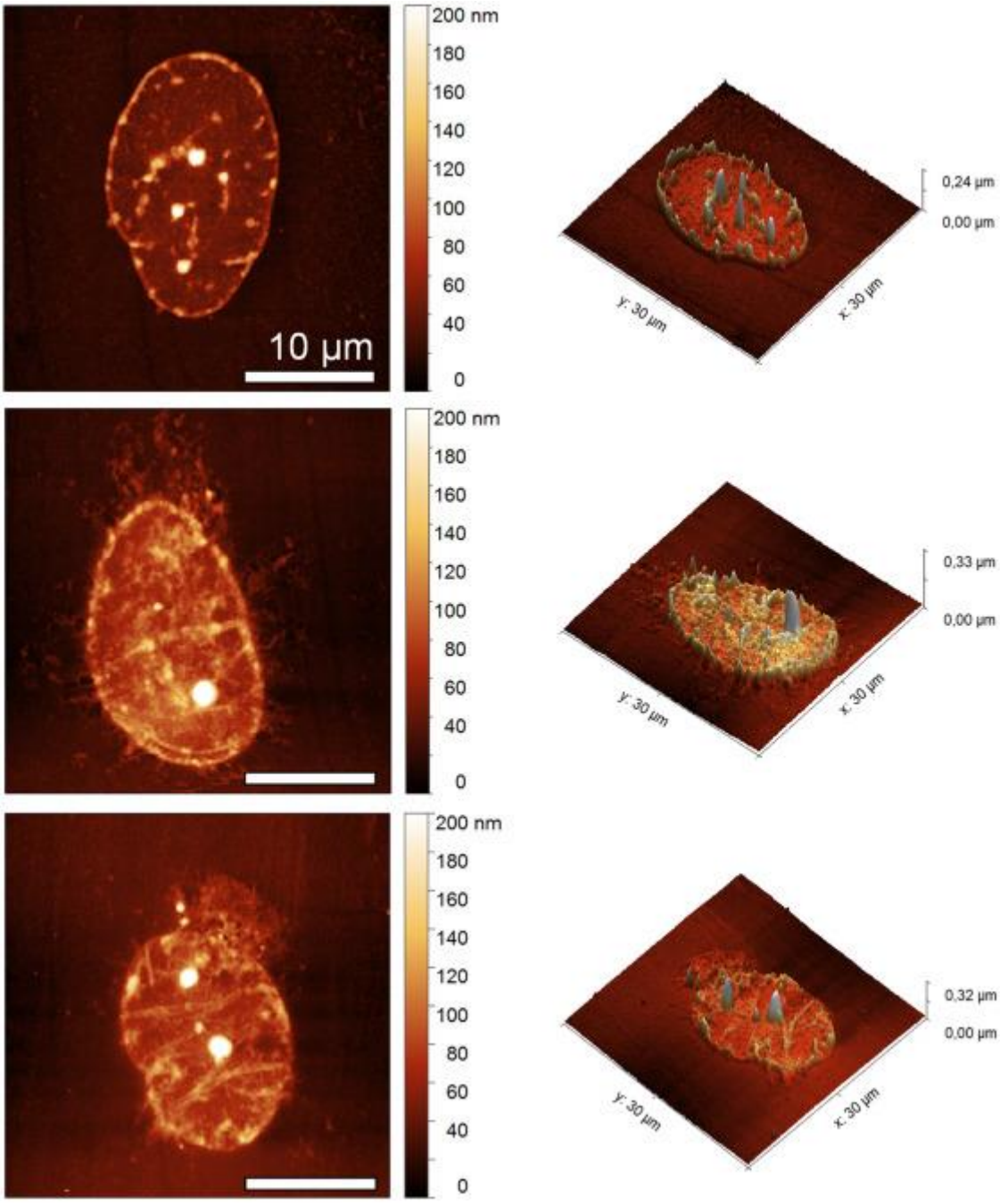

Supplementary Figure 1. AFM images of human embryo lung diploid fibroblasts nuclei subjected mechanical stress (top view on the left and 3D view on the right).

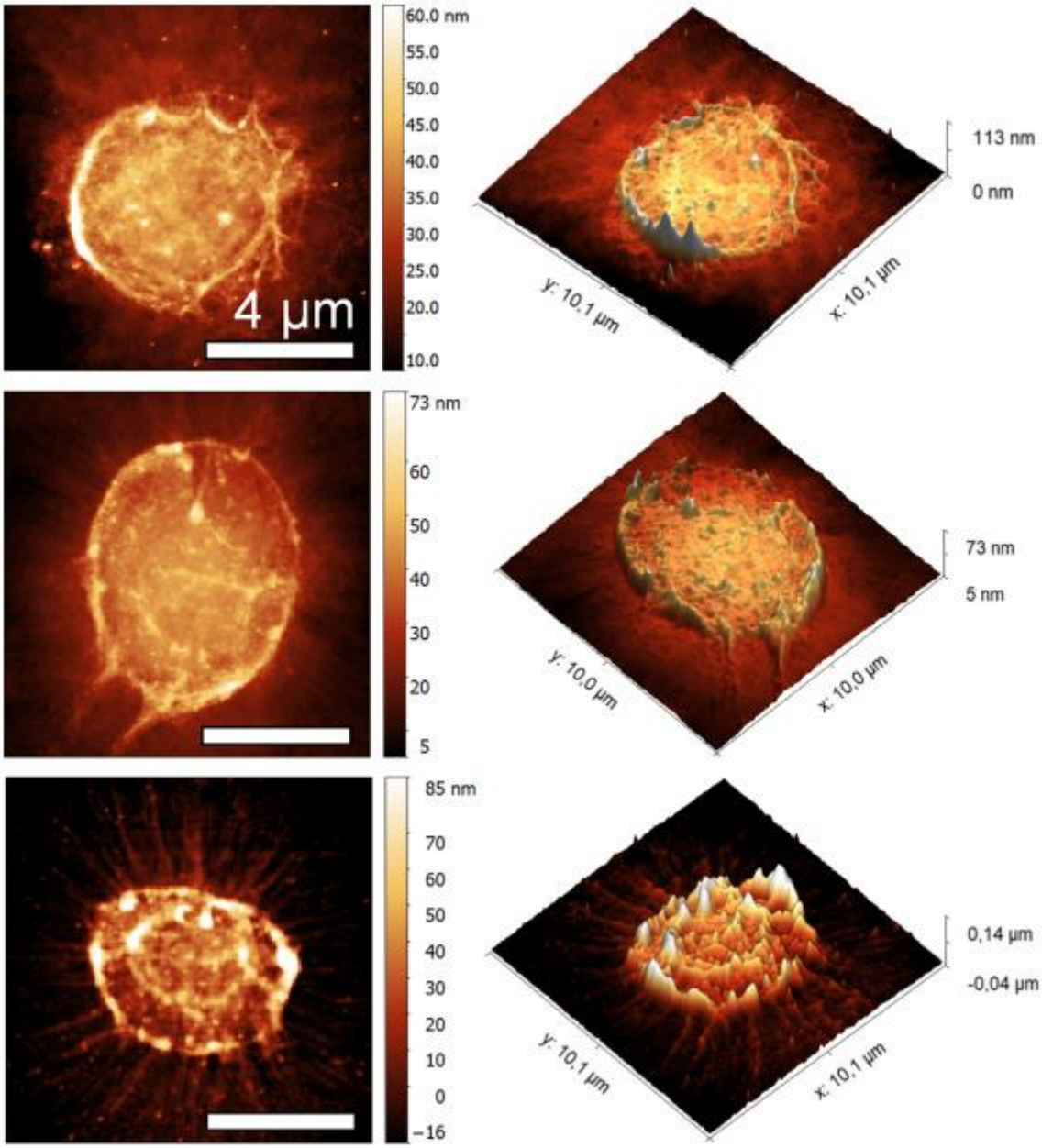

Supplementary Figure 2. AFM images of chicken erythrocytes nuclei subjected mechanical stress (2D view on the left and 3D view on the right).

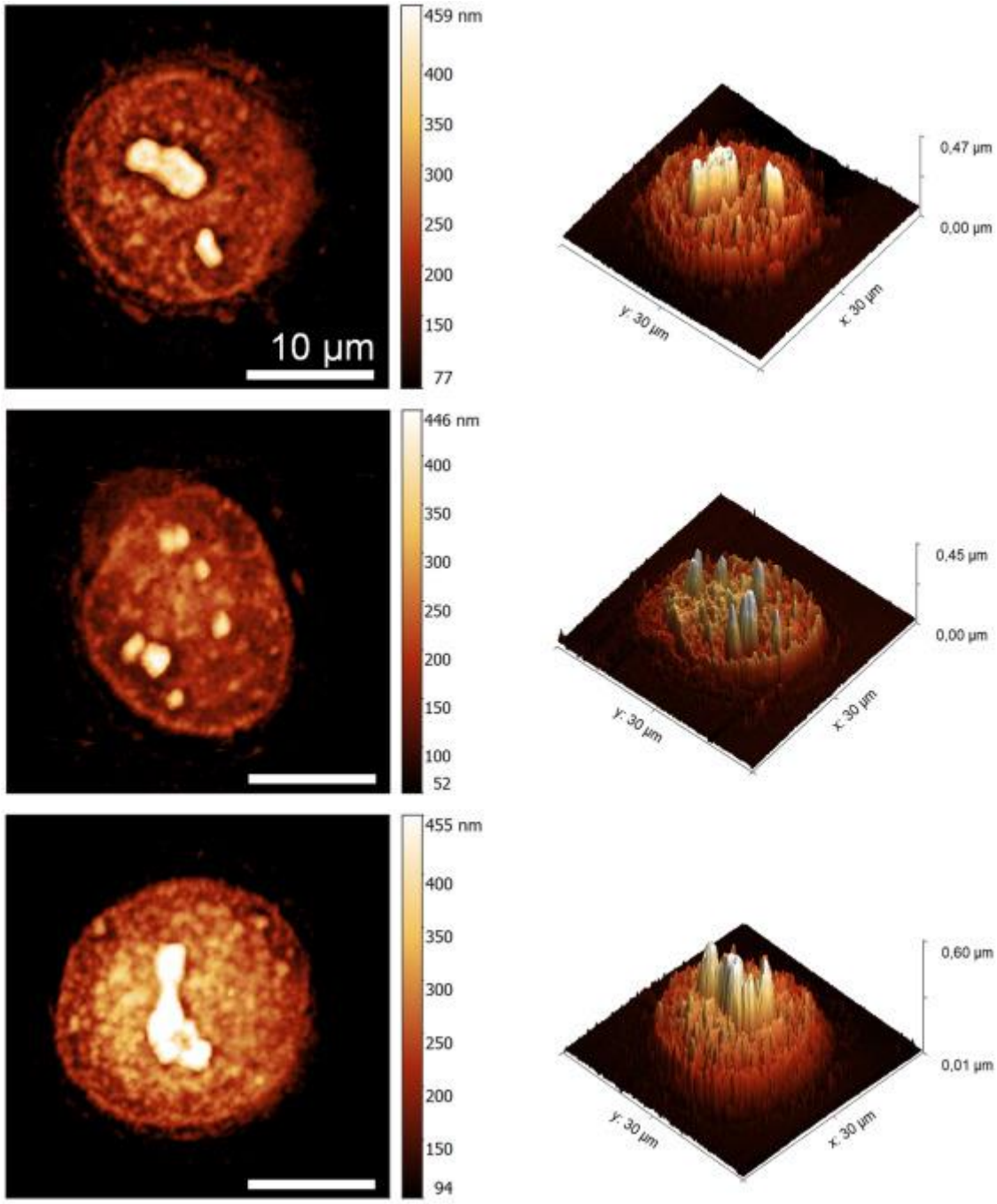

Supplementary Figure 3. AFM images of HeLa nuclei subjected mechanical stress (2D view on the left and 3D view on the right).

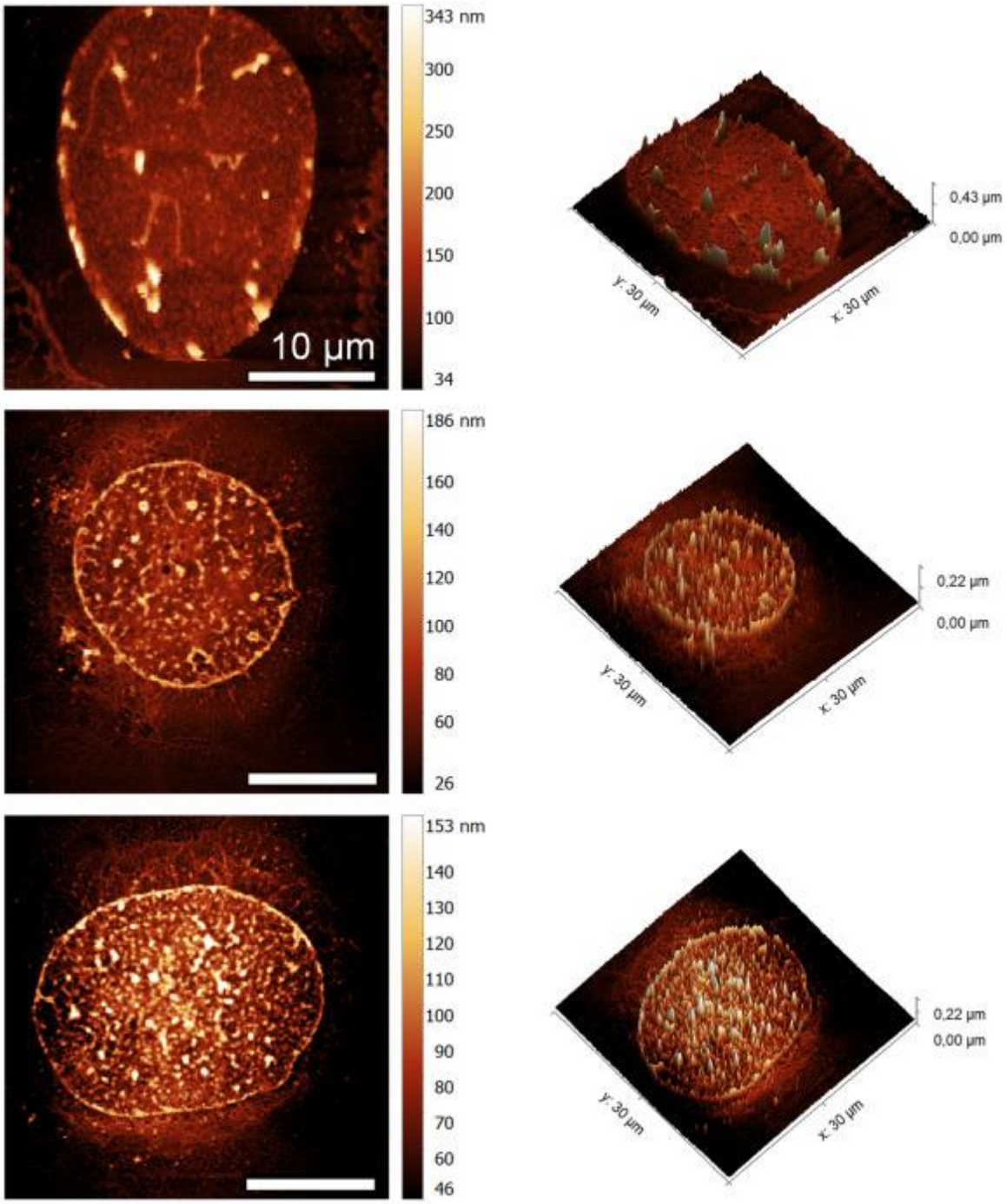

Supplementary Figure 4. AFM images of HeLa nuclei subjected mechanical stress (2D view on the left and 3D view on the right). Before nuclei isolation, HeLa cells were treated with actinomycin D in concentration of 0.12 µg/ml for 2 days.

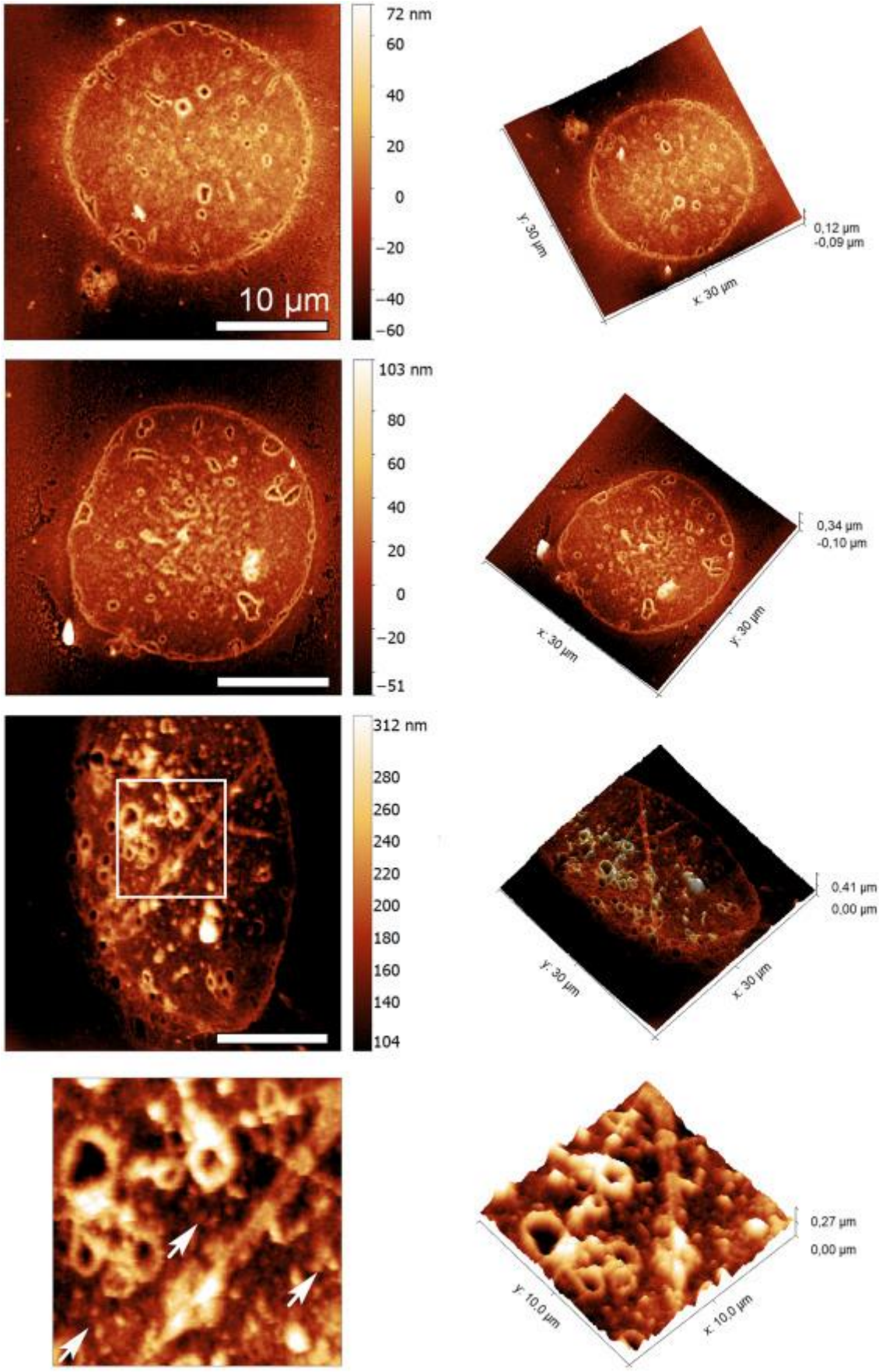

Supplementary Figure 5. AFM images of HeLa nuclei subjected mechanical stress (2D view on the left and 3D view on the right). Before nuclei isolation, HeLa cells were treated with actinomycin D in concentration of 0.12

μg/ml for 1 day. The enlarged image shows the area where both nanoloops (white arrows) and 400 nm globules are presented.

Supplementary Figure 6. Recovery of transcription after elimination of actinomycin D treatment. A complete medium with actinomycin D was replaced with a complete medium without it, SmartFlare™ probes (Merck Millipore, Germany) were added and the fluorescence dynamic of the sample was observed during the day (a confocal microscope Leica TCS SP5X SP5 (Leica, Germany) was used)